

Supporting Information

Engineering DszC mutants from transition state
macro-dipole considerations and evolutionary
sequence analysis

*Rui P. P. Neves, Maria J. Ramos, Pedro A. Fernandes**

LAQV, REQUIMTE, Departamento de Química e Bioquímica, Faculdade de Ciências,
Universidade do Porto, Rua do Campo Alegre, s/n, 4169-007 Porto, Portugal

*E-mail for P.A.F.: pafernan@fc.up.pt.

INDEX

MODELING OF THE QM/MM MODEL OF THE DSZC:DBT COMPLEX.....	2
TRANSITION STATE MACRODIPOLE CALCULATIONS WITH DIFFERENT DENSITY FUNCTIONALS AND BASIS SETS	3
POSITIONAL CONSERVATION SCORES OBTAINED FROM THE CONSURF SERVER.....	8
REFERENCES	16

Modeling of the QM/MM model of the DszC:DBT complex

The DszC:DBT complex was modelled in the catalytically-competent homodimeric form (chain A and F, with 417 residues each, from PDB ID 3X0Y with 2.3 Å resolution), in complex with the FMN cofactor in the oxidized form and with all X-ray waters within 6 Å of each catalytic site.¹ The FMN cofactor was modelled as C^{4a}-hydroperoxyflavin intermediate (C^{4a}OOH), as there was a well-defined electronic density for FMN in the active site of DszC that suggested a tight-binding of FMN to the active site of DszC. The binding pose of DBT was modelled as in the TdsC homolog enzyme from *Paenibacillus sp.* (64% identity and identical active site residues) binding oxidized FMN and DBT (PDB ID: 5XDE),² after aligning the conserved FMN cofactor and the backbone of catalytic residues His92, Ser163, His391 of both DszC and TdsC. As predicted by the Propka3.1 program,³ physiological protonation states were attributed to all residues except His92, His388 and His391: His92 and His388 were protonated as δ -tautomers and His391 was doubly-protonated as in the imidazolium form.

The DszC homodimer was described with the ff10 force field⁴, whereas DBT and C^{4a}OOH were parameterized with the GAFF⁵ and with RESP charges derived after geometry optimization of each molecule at the HF/6-31G* level – using the Antechamber module available in AMBER12 and the Gaussian software for QM calculations⁶. The Xleap module of AMBER12 was used to add 33 Na⁺ ions to counteract the overall positive charge of the system, and to add TIP3P waters⁷ to fill a rectangular box with faces at a minimum distance of 12 Å from the solute. Afterwards, a four-step molecular mechanics (MM) energy minimization protocol was applied to remove bad contacts in the system: (1) positional harmonic restraints of 50 kcal·mol⁻¹ were applied to water molecules; (2) positional harmonic restraints of 50 kcal·mol⁻¹ were applied to all heavy atoms; (3) positional harmonic restraints of 10 kcal·mol⁻¹ were applied backbone atoms of the solute; and (4) no restraints were applied.

The QM/MM model proceeding for ONIOM calculations was taken from the final minimized structure of the MM protocol. It comprised one monomer binding C^{4a}OOH and DBT, all residues of the second monomer within a radius of 18 Å from the His92, Tyr96, Asn129, Ser163, His388 and His391, C^{4a}OOH and DBT in the first monomer, and the water molecules at least 6 Å away from the catalytic site – in a total of 7238 atoms and total charge of -15. The QM layer included all atoms of DBT, the isoalloxazine ring (except for the two methyl groups in the phenyl moiety), the N¹⁰-bound hydroxymethyl of the ribitol tail of C^{4a}OOH, and the side chains of residues His92, Tyr96, Asn129, Ser163, His388 and His391 – a total of 112 atoms, zero total charge and singlet multiplicity – whereas the MM layer comprised all the remaining atoms of the model. All atoms beyond a radius of 15 Å from the molecules composing the QM layer were kept rigid throughout the ONIOM calculations. All ONIOM calculations were ran with the Gaussian software.

All QM/MM calculations were carried out at the B3LYP/6-31G(d):ff10 level of theory,⁸⁻¹⁶ with the Coulomb QM/MM interactions calculated with the electrostatic embedding scheme, as implemented in Gaussian 09.⁶ The B3LYP/6-31G(d) level has been successfully employed in other QM/MM studies of the catalytic mechanism of enzymes.¹⁷⁻²⁰ In particular, to study the triplet-singlet spin inversion taking place upon formation of the C^{4a}OOH, we allowed break of the symmetry of the singlet configuration by accepting the inclusion of imaginary coefficients and/or mixed-spin orbitals in the wavefunction.²¹⁻²³ We used hydrogens as link atoms to complete the valence of the bonds in the boundary of the two layers.²⁴⁻²⁷

Transition state macrodipole calculations with different density functionals and basis sets

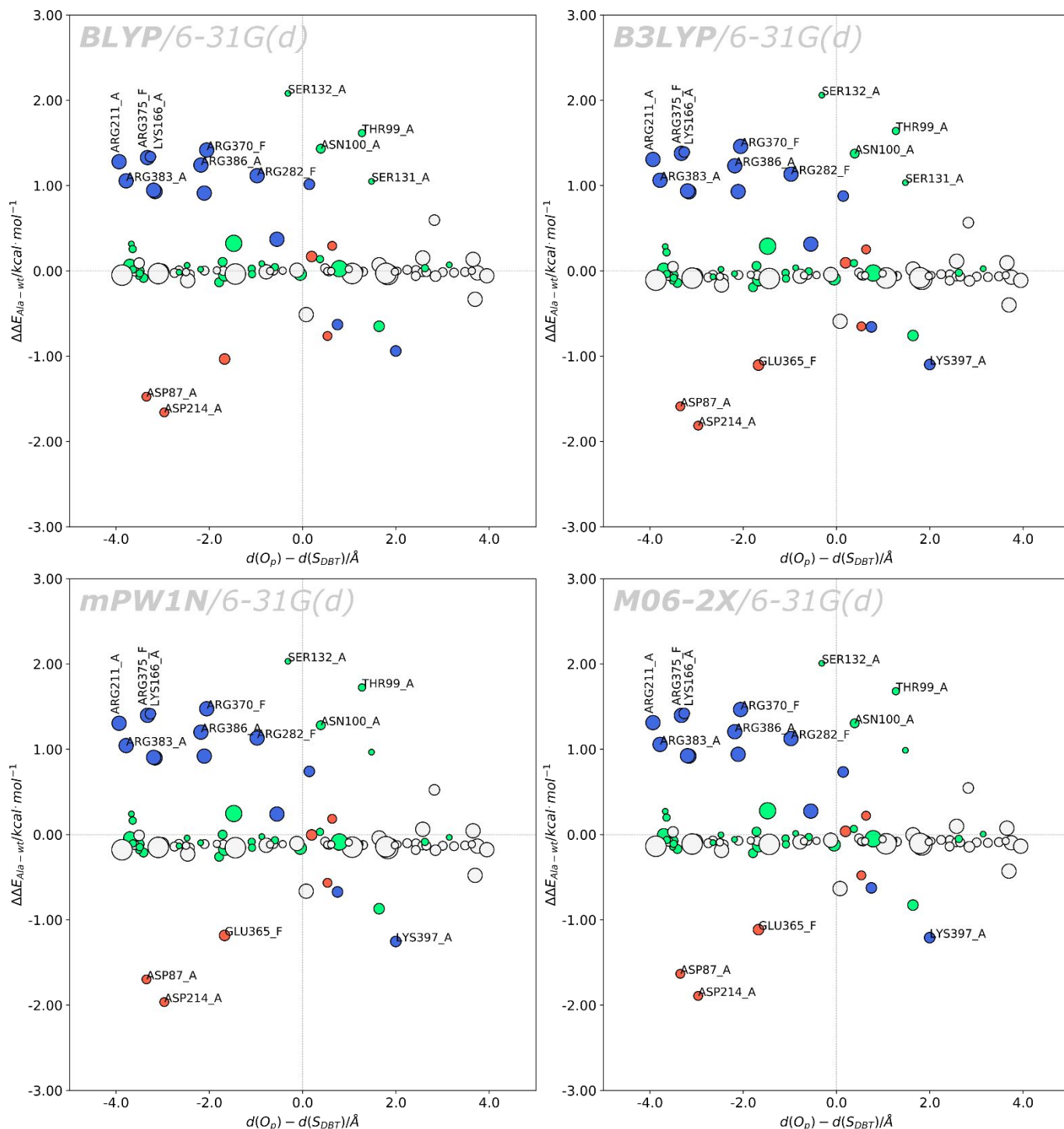


Figure S1. Activation energy differences upon alanine mutation for different density functionals (BLYP, B3LYP, mPW1N and M06-2X) as a function of the relative proximity of each residue to the O_p and the S_{DBT} atoms. Activation energy differences are calculated relatively to the activation energy of the wild-type form at the same level of theory; to determine the representative position of charged residues, only the heavy atoms of the charged group were considered to describe the position of the residue relatively to the active site, whereas the heavy atoms of the whole sidechain were considered for the remaining residues. Larger markers represent bulkier amino acids. Residues whose mutation provides a change larger than $|\Delta\Delta E_{\text{Ala-wt}}| > 1.0$ kcal·mol⁻¹ in the activation energy are labelled. Residues colored in blue and red correspond to positively and negatively charged residues, and those colored in green and gray correspond to polar and apolar residues. All calculations were performed at the ONIOM(DFT/6-31G(d):AMBER) level of theory.

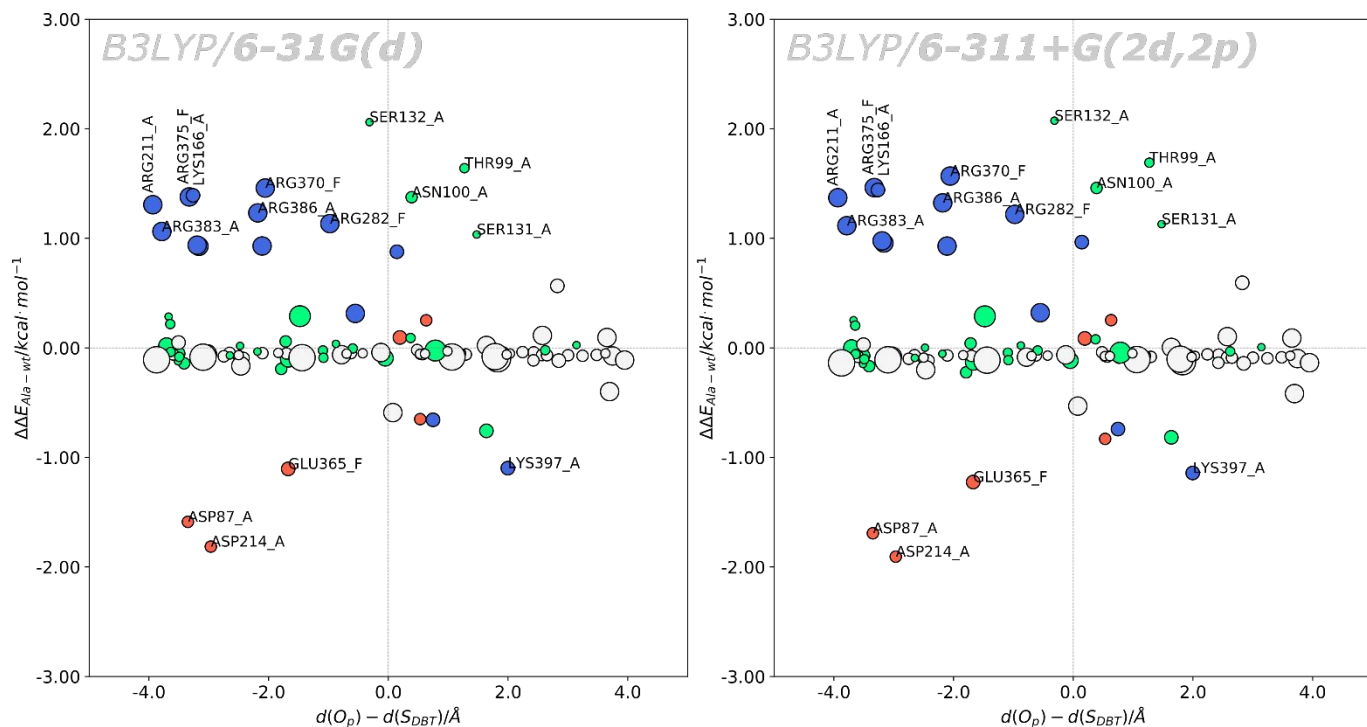
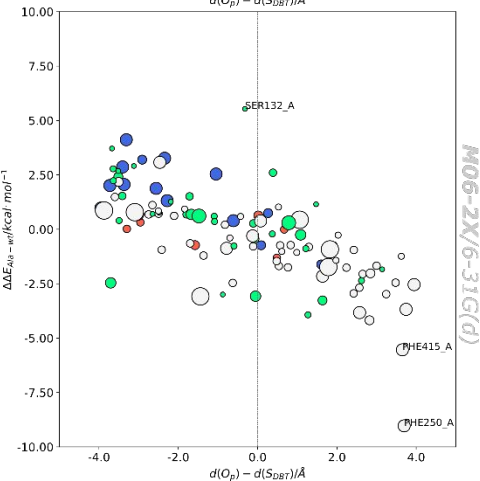
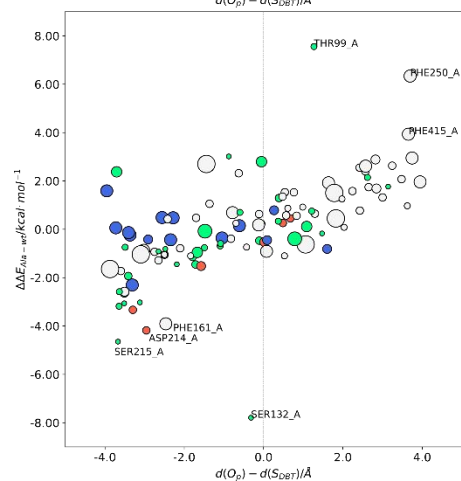
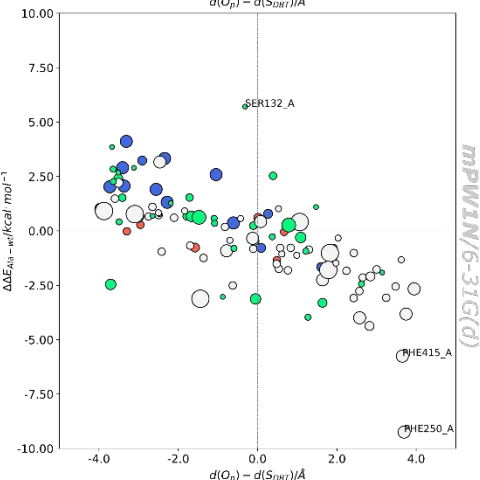
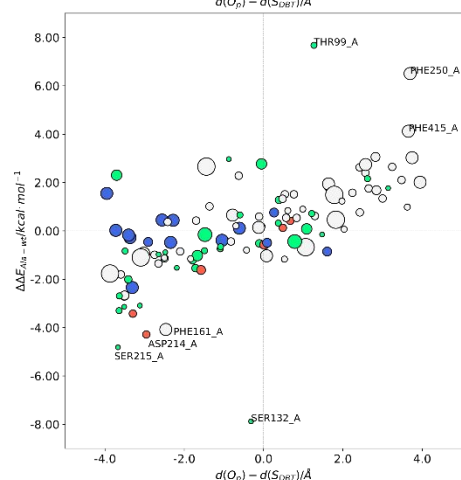
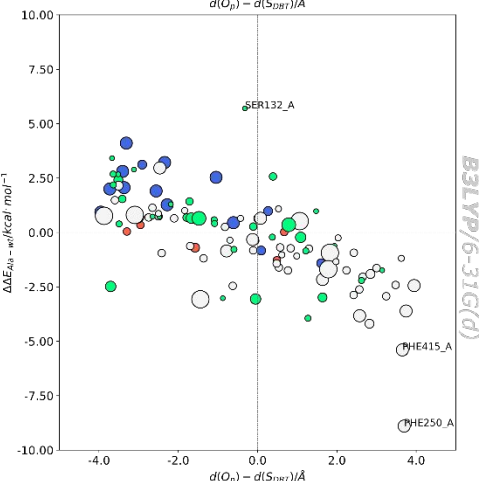
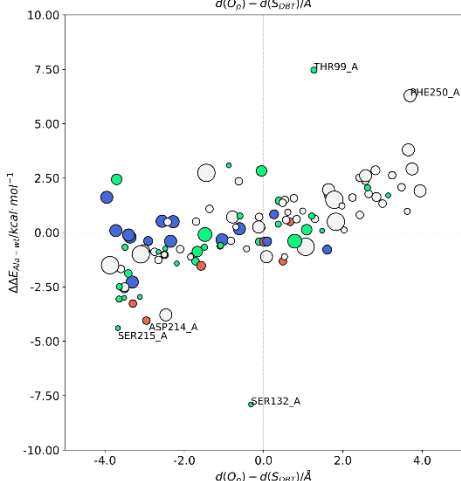
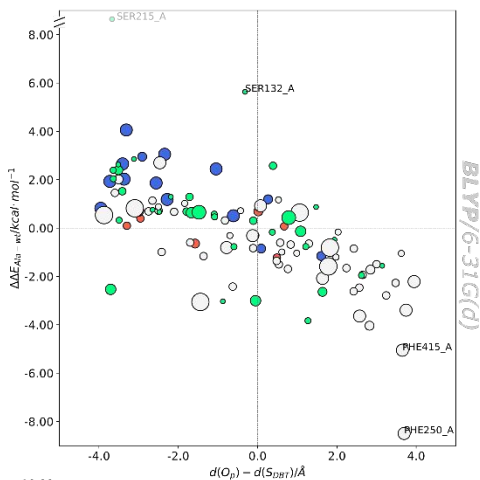
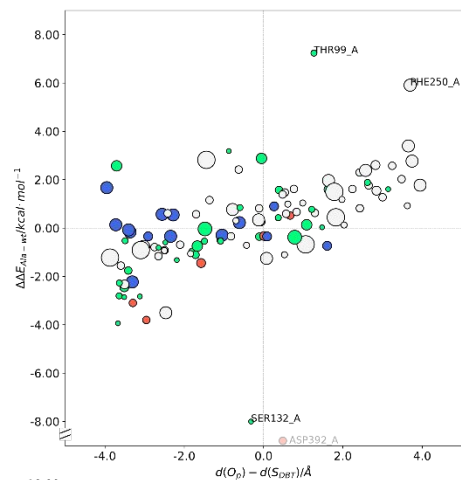


Figure S2. Activation energy differences upon alanine mutation for different basis sets (6-31G(d) and 6-311+G(2d,2p)) as a function of the relative proximity of each residue to the O_p and the S_{DBT} atoms. Activation energy differences are calculated relative to the activation energy of the wild-type form at the same level of theory; to determine the representative position of charged residues, only the heavy atoms of the charged group were considered to describe the position of the residue relative to the active site, whereas the heavy atoms of the whole sidechain were considered for the remaining residues. Larger markers represent bulkier amino acids. Residues whose mutation provides a change larger than $|1.0 \text{ kcal}\cdot\text{mol}^{-1}|$ in the activation energy are labelled. Residues colored in blue and red correspond to positively and negatively charged residues, and those colored in green and gray correspond to polar and apolar residues. All calculations were performed at the ONIOM(B3LYP:AMBER) level of theory.

A. insertion of +1e probe

B. insertion of -1e probe



BLYP/6-31G(d)

B3LYP/6-31G(d)

MPW1N/6-31G(d)

M06-2X/6-31G(d)

Figure S3. Activation energy differences for different density functionals (BLYP, B3LYP, mPW1N and M06-2X) upon insertion of a unitary probe charge in the geometric centre of the sidechain of the residues within 10 Å of the active site of DszC, as a function of the distance of the sidechain centre of mass to the O_p and S_{DBT} atoms. Larger markers represent bulkier amino acids. Since most residues are composed of C, N and O, we assumed for simplicity that the geometric center of each sidechain should closely resemble their centre of mass. Residues in which the probe insertion leads to a change larger than 50% of the maximum energy difference relative to the activation energy are labelled. Residues colored in blue and red correspond to positively and negatively charged residues, and those colored in green and gray correspond to polar and apolar residues.

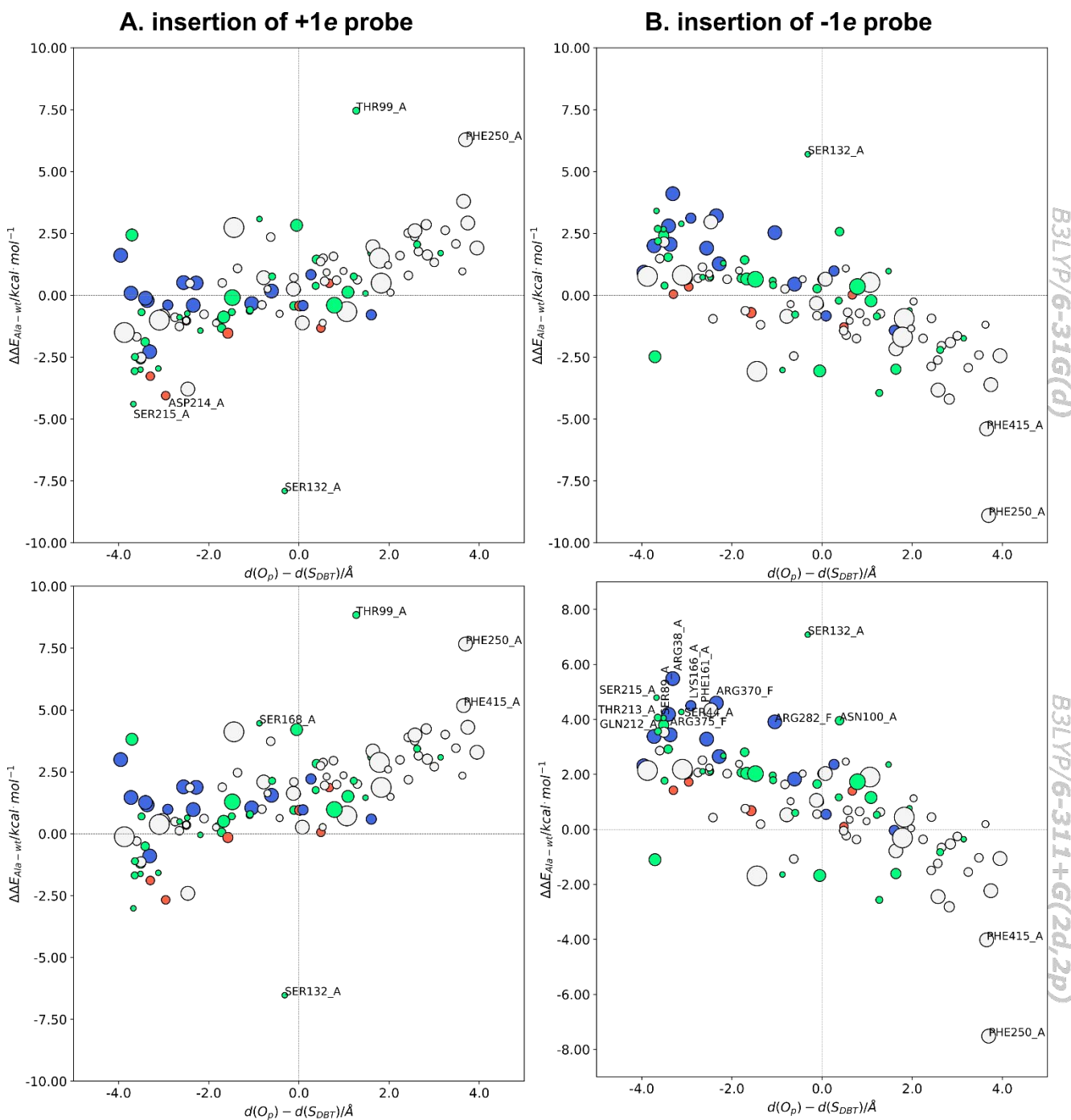


Figure S4. Activation energy differences for different basis sets (6-31G(d) and 6-311+G(2d,2p)) upon insertion of a unitary probe charge in the geometric centre of the sidechain of the residues within 10 Å of the active site of DszC, as a function of the distance of the sidechain centre of mass to the O_p and S_{DBT} atoms. Larger markers represent bulkier amino acids. Since most residues are composed of C, N and O, we assumed for simplicity

that the geometric center of each sidechain should closely resemble their centre of mass. Residues in which the probe insertion leads to a change larger than 50% of the maximum energy difference relative to the activation energy are labelled. Residues colored in blue and red correspond to positively and negatively charged residues, and those colored in green and gray correspond to polar and apolar residues.

Positional conservation scores obtained from the ConSurf server

	pos	ALA	CYS	ASP	GLU	PHE	GLY	HIS	ILE	LYS	LEU	MET	ASN	PRO	GLN	ARG	SER	THR	VAL	TRP	TYR	MAX AA	ConSurf Grade		
MET	1										100.0											M 100.000	6*		
THR	2																	100.0					T 100.000	8*	
LEU	3									100.0													L 100.000	7*	
SER	4																40.0	60.0					T 60.000	7*	
PRO	5													80.0					20.0				P 80.000	6*	
GLU	6	20.0			40.0									20.0					20.0				E 40.000	3*	
LYS	7			20.0				20.0		40.0						20.0							K 40.000	3*	
GLN	8					20.0									40.0				20.0		20.0		Q 40.000	1*	
HIS	9							50.0							16.7		16.7	16.7					H 50.000	4*	
VAL	10			12.5			12.5				12.5								25.0	37.5			V 37.500	2*	
ARG	11	20.0						10.0		10.0						40.0	10.0	10.0					R 40.000	2*	
PRO	12	16.7		8.3										66.7				8.3					P 66.667	5	
ARG	13	25.0		12.5			6.3							6.3	6.3	25.0			12.5		6.3		AR 25.000	1	
ASP	14	18.2		9.1		4.5	4.5				9.1		4.5	36.4	4.5	4.5			4.5				P 36.364	1	
ALA	15	53.3		3.3	3.3		3.3	3.3						10.0		6.7	16.7						A 53.333	5	
ALA	16	20.5		28.2	7.7		2.6								2.6	7.7	7.7	20.5	2.6				D 28.205	3	
ASP	17	12.2		34.1	4.9	2.4	2.4	4.9			7.3		2.4	4.9	4.9	7.3	4.9	7.3					D 34.146	1	
ASN	18	32.1		9.4	5.7	3.8				5.7			9.4	7.5	9.4	1.9	5.7	5.7	1.9		1.9		A 32.075	1	
ASP	19	4.7		40.6	20.3		4.7	3.1					4.7	3.1	3.1	1.6	6.3	7.8					D 40.625	4	
PRO	20	25.4				1.5		1.5	3.0		3.0			29.9				1.5		1.5	26.9	6.0	P 29.851	3	
VAL	21	1.4		1.4		2.7			20.5		57.5		1.4		1.4	1.4			9.6	2.7			L 57.534	2	
ALA	22	52.1		6.4	6.4		1.1	1.1		1.1	2.1		1.1	2.1	9.6	8.5	3.2	3.2	2.1				A 52.128	4	
VAL	23	8.9		1.0					17.8	5.0	4.0	1.0		1.0	3.0	15.8	4.0	9.9	28.7				V 28.713	3	
ALA	24	84.2				0.9			0.9		4.4							1.8	7.9				A 84.211	8	
ARG	25	16.4		12.3	13.9		3.3	3.3	1.6	3.3					11.5	26.2	2.5	4.1	1.6				R 26.230	1	
GLY	26	19.4		11.6	27.9	1.6	2.3	0.8		3.1	3.1				8.5	9.3	10.9	1.6					E 27.907	1	
LEU	27	3.7				0.7			3.0		56.3	0.7							2.2	33.3			L 56.296	7	
ALA	28	74.6	0.7				0.7		3.6		2.2					6.5	6.5	1.4	3.6				A 74.638	7	
GLU	29	36.7		18.0	17.3		0.7	0.7		1.4	0.7		1.4	2.2	10.1	4.3	2.2	2.9	1.4				A 36.691	1	
LYS	30	12.7		8.5	21.8		1.4	1.4	7.7	4.2	2.8		0.7		7.0	12.7	2.1	8.5	7.7		0.7		E 21.831	1	
TRP	31	0.7				33.8			2.1		61.3										2.1			L 61.268	7
ARG	32	59.4		1.4	2.8		0.7	2.1		0.7					0.7	22.4	4.2	3.5	0.7		1.4		A 59.441	6	
ALA	33	34.2		0.7	10.3				1.4	6.8	6.2			4.1	4.8	9.6	3.4	8.9	9.6				A 34.247	1	
THR	34			32.7			7.5							2.7		4.1	8.8	44.2					T 44.218	7	
ALA	35	93.9					1.4		0.7		0.7					0.7			2.7				A 93.878	9	
VAL	36	35.6	0.7	0.7	0.7		1.3		2.0		7.4		1.3	4.0			4.7	0.7	40.9				V 40.940	4	
GLU	37	22.8		4.7	51.0		0.7	1.3		2.0	2.7				5.4	1.3	0.7	4.0	3.4				E 51.007	3	
ARG	38										4.7						95.3						R 95.302	9	
ASP	39			92.6	7.4																		D 92.617	9	
ARG	40	9.4			4.0			2.7	1.3	13.4	1.3				14.8	51.0	0.7	0.7			0.7		R 51.007	4	
ALA	41	41.6		2.7	16.8		0.7	0.7	0.7	4.7	5.4				10.7	10.7	1.3	2.7	1.3				A 41.611	3	
GLY	42	3.4		0.7			66.4				0.7			19.5		0.7	8.1		0.7				G 66.443	7	
GLY	43	14.8			0.7		52.3		0.7	12.1	4.0				3.4	10.7		0.7	0.7				G 52.349	6	
SER	44	6.0		2.7	2.7			16.8	0.7		8.7		4.0	9.4	1.3	5.4	9.4	30.9	1.3		0.7		T 30.872	6	
ALA	45	27.5												72.5									P 72.483	8	
THR	46	14.1	0.7	1.3	1.3	8.7		4.0		20.8	10.1				1.3	16.1	2.7	6.0	6.7	1.3	4.7		K 20.805	1	
ALA	47	47.7		10.7	9.4	2.0	1.3	3.4	2.0	3.4	1.3		1.3	1.3	4.0	4.7	2.0	2.0	2.0		1.3		A 47.651	1	
GLU	48	2.0		0.7	89.9						0.7				6.7								E 89.933	9	
ARG	49	2.7						20.8	6.0	9.4						38.3			22.8				R 38.255	7	
GLU	50	14.8		26.8	22.1		2.0		1.3	0.7				1.3	14.8	8.1	4.0	1.3	2.7				D 26.846	3	
ASP	51	10.7		1.3	1.3			1.3	0.7	4.0	54.4	1.3			1.3	15.4	0.7	0.7	0.7	6.0			L 54.362	4	
LEU	52				2.7			23.5			72.5	0.7							0.7				L 72.483	7	
ARG	53	4.7								25.5						61.7	6.7	1.3					R 61.745	8	
ALA	54	20.8		20.1	18.1		2.0	8.7		3.4			4.0		14.8	4.7	2.0	0.7			0.7		A 20.805	1	

Table S1. Per residue variety for each position in the

sequence of DszC, after the multi-sequence analysis performed by the ConSurf server

SER	55	22.1		0.7		0.7	3.4		1.3		1.3		1.3		67.8		0.7	0.7	S 67.785	7		
GLY	56		4.0			94.6		0.7						0.7					G 94.631	9		
LEU	57								100.0										L 100.000	9		
LEU	58	0.7				0.7			81.2	1.3	2.0	0.7			2.7	9.4	1.3		L 81.208	8		
SER	59	18.9	2.7	1.4		7.4	0.7	10.1	1.4	7.4	3.4	3.4	4.1	12.2	26.4			0.7	T 26.351	2		
LEU	60	8.1		1.4			5.4		68.9	0.7						15.5			L 68.919	7		
LEU	61	17.8			0.7	2.7		4.8	33.6	1.4			2.7	21.9	11.0	2.7	0.7		L 33.562	6		
VAL	62	2.7	1.4	4.1	0.7	14.4	4.8	38.4	2.7	0.7				0.7	2.7	26.7			I 38.356	6		
PRO	63	6.8				0.7			0.7		89.7			1.4			0.7		P 89.726	8		
ARG	64	22.6	0.7		3.4	3.4	0.7	17.1		0.7	6.2	2.7	21.2	0.7	10.3	10.3			A 22.603	2		
GLU	65	21.9	0.7	3.4	47.9	0.7	0.7	6.2		0.7	0.7	10.3	3.4	2.1	0.7		0.7		E 47.945	3		
TYR	66	2.1		0.7	21.9		21.2	4.8	9.6	0.7				0.7		2.1	1.4	34.9	Y 34.932	2		
GLY	67		0.7			98.6								0.7					G 98.630	9		
GLY	68		0.7			99.3													G 99.315	9		
TRP	69	19.2	2.7	4.8	0.7	26.7	4.8	0.7	13.0	0.7	0.7	0.7	13.0	1.4	3.4	1.4	0.7	3.4	2.1	G 26.712	1	
GLY	70	2.1	6.8	11.6		76.0		0.7		0.7		1.4		0.7					G 76.027	5		
ALA	71	40.5		7.4		8.1	1.4	0.7	0.7	14.2			17.6		0.7	0.7	7.4	0.7	A 40.541	5		
ASP	72	2.0	26.2	2.7		6.0	2.0				9.4	15.4	0.7	7.4	20.8	7.4			D 26.174	1		
TRP	73	4.0			2.7		1.3		4.0			0.7	1.3		0.7	0.7	79.2	5.4	W 79.195	7		
PRO	74	13.4	3.4	5.4		2.7	2.0	2.7	2.0	4.7		20.1	8.1	3.4	18.1	5.4	8.7		P 20.134	1		
THR	75	3.4	12.1	11.4	0.7			2.7	7.4		0.7		10.7	1.3	2.7	38.3	8.7		T 38.255	4		
ALA	76	30.2			2.0	9.4		17.5	10.7	0.7			1.3		2.0	16.1	10.1		A 30.201	6		
ILE	77	7.4	0.7		11.4		2.7	1.3	35.6	2.0	0.7		4.0		1.3	1.3	1.3	30.2	L 35.570	4		
GLU	78	10.1	4.0	17.5		3.4	4.0		14.8	2.7		1.3		13.4	26.8	1.3	0.7		R 26.846	2		
VAL	79	10.7	0.7			1.3	1.3	25.5		8.7						8.7	43.0		V 42.953	4		
VAL	80	1.3			6.0	1.3		26.2	4.0	0.7				3.4	7.4	49.7			V 49.664	5		
ARG	81	1.3				0.7		0.7					3.4	93.3		0.7			R 93.289	9		
GLU	82	5.4		31.5		0.7	0.7	18.1	2.0	8.7			4.0	21.5		4.7	2.7		E 31.544	3		
ILE	83				18.8			30.9	28.2	2.0							20.1		I 30.872	5		
ALA	84	88.6				3.4									8.1				A 88.591	9		
ALA	85	22.1		4.0				18.8					8.7	36.9	5.4	3.4	0.7		R 36.913	4		
ALA	86	40.3				19.5			0.7					1.3	5.4	32.9			A 40.268	6		
ASP	87		95.3	4.7															D 95.302	9		
GLY	88	8.1				36.2					3.4			47.0	5.4				S 46.980	8		
SER	89	18.8								2.0				79.2					S 79.195	9		
LEU	90	0.7			0.7			43.0	40.9	0.7				0.7		13.4			I 42.953	6		
GLY	91	61.7				38.3													A 61.745	8		
HIS	92						59.7			6.7			33.6						H 59.732	9		
LEU	93						9.4		65.1							25.5			L 65.101	7		
PHE	94			29.5			3.4		44.3			8.1				2.7	12.1		L 44.295	6		
GLY	95	19.5				66.4			1.3			8.1		3.4	0.7	0.7			G 66.443	6		
TYR	96		2.0			36.9		0.7			6.0			5.4			49.0		Y 48.993	8		
HIS	97						82.6			0.7		15.4			1.3				H 82.550	8		
LEU	98		2.7			16.1		35.6	1.3	10.7			1.3		0.7	0.7	30.9		H 35.570	6		
THR	99	5.4			3.4	2.0	0.7	0.7	65.8		1.3			4.7	2.0	13.4	0.7		L 65.772	6		
ASN	100		2.0			3.4	4.0		13.4	11.4	12.1	4.0	26.8		2.0		14.8	6.0	Q 26.846	6		
ALA	101	6.0		0.7	2.7	3.4		10.1	28.9	0.7	1.3		3.4		17.5	3.4	22.1		L 28.859	6		
PRO	102	34.2	0.7	0.7	0.7	2.0	2.0	4.0	0.7	1.3		8.1	1.3	7.4	4.0	0.7	8.1	9.4	14.1	0.7	A 34.228	5
MET	103	9.4			0.7	4.7	0.7	7.4	3.4	2.0	6.0			4.0	15.4	30.2	8.1	3.4	4.7	T 30.201	6	
ILE	104	22.1			0.7	2.0		18.1	7.4	0.7		9.4			2.7	6.0	30.9		V 30.872	4		
GLU	105	4.0	5.4	6.0		4.7	8.7	2.0	10.7	0.7	6.0		7.4	30.2	3.4	2.0	2.7		6.0	R 30.201	2	
LEU	106	1.3			9.4	0.7		10.7	51.0	0.7				6.7		1.3	10.7	7.4		L 51.007	6	
ILE	107	6.7		0.7	36.9	1.3	0.7	0.7	5.4	0.7			6.0	4.7	2.7	1.3	16.1	4.7	11.4	F 36.913	5	
GLY	108	15.3	2.0	1.3	0.7	70.7		0.7	2.0					0.7	0.7	4.7	0.7	0.7		G 70.667	5	
SER	109	3.4	5.4	4.0		3.4		0.7	1.3		7.4	0.7	4.0	11.4	22.8	34.2	1.3		T 34.228	3		
GLN	110	12.8	10.1	10.7		2.7	0.7	0.7	2.0		0.7	47.7	2.7	5.4	1.3	2.7			P 47.651	1		
GLU	111	31.8	8.1	45.3	0.7	2.7	1.4		0.7		0.7		3.4	1.4	1.4	1.4	1.4		E 45.270	3		
GLN	112	0.7			0.7	0.7	1.4		0.7	5.4			82.4	4.7		2.0	1.4		Q 82.432	8		
GLU	113	23.0		1.4		2.0	3.4	6.8	8.8	0.7			12.8	14.2	1.4	0.7	4.1	16.9	4.1	A 22.973	5	
GLU	114	18.2	7.4	35.8		0.7	2.7		3.4		0.7	1.4	15.5	9.5	1.4	1.4	0.7	1.4		E 35.811	1	
HIS	115	15.5	4.1	4.1	8.8		6.1		2.7	0.7		2.7	10.1	4.1	33.1	2.0	2.7	0.7	2.7	R 33.108	1	
LEU	116	0.7			18.9	0.7	1.4	8.8	20.9	0.7			0.7	0.7	0.7	2.0	7.4	25.0	11.5	W 25.000	1	

TYR	117	4.7	1.4	10.1	18.9	4.7	1.4	2.0	26.4	8.1	0.7	6.8	2.0	0.7	12.2	L 26.351	3			
THR	118	10.8	1.4	15.5	6.8	8.8	0.7	1.4	2.7	35.1	5.4	9.5	2.0			R 35.135	2			
GLN	119	10.0	4.0	22.0	1.3	11.3	2.7	1.3	2.7	11.3	0.7	2.7	11.3	16.0	0.7	0.7	1.3	E 22.000	1	
ILE	120	8.0		0.7	0.7	9.3	2.7	4.0				12.7	51.3	8.0	2.7	T 51.333	7			
ALA	121	36.7	0.7		2.7	8.7	9.3	0.7			0.7	0.7	9.3	30.7		A 36.667	5			
GLN	122	22.0	2.7	23.3	1.3	1.3	4.0	2.0	8.7	20.0	10.0	4.7				E 23.333	1			
ASN	123	2.0	1.3	18.0	0.7	18.7	10.7	8.7	2.0	22.7	0.7	9.3	4.0	1.3		N 22.667	2			
ASN	124	2.0	5.3	1.3		9.3	2.0	7.3	0.7	32.7		9.3	25.3	4.0	0.7	N 32.667	3			
TRP	125	0.7	0.7		0.7	0.7	1.3		22.0	0.7	0.7	1.3	8.0		0.7	54.7	8.0	W 54.667	4	
TRP	126		3.3		71.3		0.7	9.3								2.0	8.7	4.7	F 71.333	7
THR	127			8.0		0.7	1.4				3.6			1.4	5.8	77.5	1.4	W 77.536	8	
GLY	128	5.3	2.7		88.0							4.0							G 88.000	8
ASN	129	4.7	3.3		29.3				60.0			2.0	0.7						N 60.000	9
ALA	130	70.7			5.3		2.0					4.7	6.7	10.7					A 70.667	8
SER	131	2.7		4.7	4.0		2.0	33.3	0.7	0.7		10.0	8.7	2.7	30.7				L 33.333	6
SER	132	3.3	0.7		6.7			86.7	0.7	2.0									N 86.667	9
GLU	133	5.4		1.3	0.7				75.8		2.0	5.4	2.0	7.4					P 75.839	7
ASN	134								100.0										N 100.000	6*
ASN	135								100.0										N 100.000	6*
SER	136											100.0							S 100.000	6*
HIS	137					100.0													H 100.000	6*
VAL	138													100.0					V 100.000	6*
LEU	139	3.3		2.7	0.7		40.0	2.0	1.3	8.0	38.7		0.7	2.7					L 40.000	7
ASP	140		84.7	3.3	4.7				1.3	0.7		4.7					0.7		D 84.667	9
TRP	141	9.3	2.7	1.3	5.3		6.7	12.0	2.7	3.3	18.7	2.7	12.0	5.3	16.0	0.7	1.3		P 18.667	2
LYS	142	4.7	18.0	1.3	10.0	2.0	2.7		0.7	2.0	1.3	46.7	6.7	3.3		0.7			R 46.667	6
VAL	143	5.3	0.7	0.7	1.3	0.7	1.3	43.3				6.7	30.0	10.0					L 43.333	6
ARG	144	2.7		7.3	2.0	0.7	6.7	10.7	4.0	0.7		6.0	17.3	2.7	20.7	18.7			T 20.667	1
ALA	145	30.7	1.3		4.7		14.0	33.3	1.3				2.0		12.7				L 33.333	6
THR	146	7.3	0.7	6.0	0.7	2.0	1.3	7.3	2.0	0.7	4.0	12.0	7.3	45.3	2.7	0.7			T 45.333	3
PRO	147	8.0	10.0	10.7	0.7	1.3		7.3	1.3	0.7	22.0	3.3	24.7	6.7	1.3	0.7	1.3		R 24.667	1
THR	148	3.3	26.7	10.0	5.3	1.3	2.7	1.3	0.7	3.3	1.3	4.0	12.7	3.3	14.7	8.7	0.7		D 26.667	1
GLU	149	12.5		6.3	25.0				3.1	37.5		6.3	9.4						P 37.500	1
ASP	150	8.0	28.7	8.7	42.7		2.0		2.0	4.7	0.7		2.0	0.7					G 42.667	1
GLY	151	1.3	28.0	10.0	41.3	1.3	2.0		7.3	0.7	1.3		1.3	4.7			0.7		G 41.333	1
GLY	152	1.3	6.0	5.3	0.7	48.7	7.3	0.7	1.3		4.7	2.0	1.3	7.3	3.3		8.7	1.3	G 48.667	1
TYR	153		0.7		20.7		4.0	6.7	12.7			0.7	5.3	0.7		2.0	11.3	35.3	Y 35.333	1
VAL	154	3.3		10.7	2.0		6.7	12.7			1.3	26.7	0.7	2.0	32.7		1.3		V 32.667	1
LEU	155				27.3		5.3	52.0							11.3		4.0		L 52.000	6
ASN	156	1.3	24.0	2.0		5.3	0.7		37.3		3.3	1.3	16.0	8.0	0.7				N 37.333	5
GLY	157				100.0														G 100.000	9
THR	158	4.0	4.0	2.7	6.7		2.7	4.7	13.3	4.0	0.7	1.3	4.7	26.7	4.7	5.3	13.3	1.3	R 26.667	1
LYS	159							83.3				3.3	13.3						K 83.333	9
HIS	160	0.7			5.3	10.0	10.7		2.7	6.0		2.7	46.0	15.3				0.7	S 46.000	6
PHE	161				86.7												13.3		F 86.667	9
CYS	162	20.7	40.7		2.0				6.0				28.0	1.3	1.3				C 40.667	7
SER	163	1.3											54.7	44.0					S 54.667	9
GLY	164	2.7			96.0				1.3										G 96.000	9
ALA	165	55.3			9.3								20.7	8.7	6.0				A 55.333	7
LYS	166	8.0		0.7	2.0	9.3	4.0	8.7	18.0	1.3	1.3	0.7	2.0	10.7	13.3	3.3	16.0	0.7	L 18.000	3
GLY	167	0.7	0.7	26.0	8.0	18.7	12.0	2.7					0.7	1.3	29.3				V 29.333	6
SER	168	31.3			5.3										63.3				S 63.333	8
ASP	169		78.0	8.0		4.0					8.7		1.3						D 78.000	8
LEU	170	2.7	0.7		0.7	6.0		13.3	17.3		4.7	20.0			15.3	10.0	9.3		R 20.000	4
LEU	171					19.3		53.3	7.3	0.7		1.3	0.7	14.7	2.7				L 53.333	7
PHE	172	2.0			0.7	12.0		13.3	0.7	7.3	10.0	2.0		4.7	20.0	25.3	0.7	0.7	V 25.333	6
VAL	173	16.0	2.7		2.0		10.7	18.7							2.0	48.0			W 48.000	6
PHE	174	3.3		14.7	1.3	3.3		8.7		5.3		4.7	49.3	8.7			0.7		S 49.333	8
GLY	175	64.0			0.7	23.3		0.7	2.0						4.0	5.3			A 64.000	7
VAL	176	6.7	2.0	4.0	2.0	6.0	6.0	6.0		2.0	6.0	8.7	4.7	7.3	24.7	8.7	5.3		V 24.667	1
VAL	177				10.0		20.0	30.0							10.0	30.0			LV 30.000	2*
GLN	178	20.0		20.0	20.0						40.0								Q 40.000	4*

ASP	179				66.7														33.3		D 66.667	6*		
ASP	180					60.0				40.0											D 60.000	5*		
SER	181	7.5			25.6	2.3	1.5	4.5	10.5	1.5	3.8	15.8	0.8	5.3	0.8	3.8	7.5	1.5	4.5	1.5	1.5	D 25.564	1	
PRO	182	10.9			10.9	35.7		3.9		0.8	3.1			1.6	13.2	6.2	1.6	5.4	3.9	2.3	0.8	E 35.659	2	
GLN	183	12.1			22.7	9.1	3.0	20.5	1.5	0.8	1.5	6.1		3.0	3.8	1.5	0.8	6.1	3.8	3.0	0.8	D 22.727	1	
GLN	184	6.8	1.5		11.3	3.0		14.3	2.3	1.5		0.8		3.0	3.8	2.3	1.5	10.5	36.1	1.5		T 36.090	1	
GLY	185	4.0			21.5	8.1		46.3			2.0			3.4		5.4	2.0	5.4	2.0			G 46.309	1	
ALA	186	12.0			10.7	15.3		5.3			19.3			3.3		8.7	14.0	4.7	6.0	0.7		K 19.333	1	
ILE	187	4.7			0.7		4.0	0.7	14.7	6.0	4.0	36.0	0.7		12.7		9.3	0.7	1.3	4.7		L 36.000	4	
ILE	188	6.7						6.0	14.7			30.0					3.3	0.7	1.3	32.0	2.7	2.7	V 32.000	4
ALA	189	6.0				28.7	2.0	1.3	21.3			5.3	1.3	2.7		0.7		2.7	8.0	18.0	2.0	F 28.667	4	
ALA	190	57.3				11.3	9.3					11.3						0.7	1.3	7.3	1.3	A 57.333	6	
ALA	191	29.3	0.7			4.7		1.3	12.0			7.3				2.0		3.3	2.7	30.0	6.7	V 30.000	4	
ILE	192	1.3						30.7			17.3								0.7	50.0		V 50.000	6	
PRO	193	1.3			9.3	3.3				2.7				82.0		0.7			0.7			P 82.000	7	
THR	194	13.3				0.7		6.0	0.7		2.7	0.7		4.0		8.7	13.3	49.3		0.7		T 49.333	5	
SER	195	9.3			28.7	2.7	0.7	14.7	2.0	0.7	3.3	0.7		8.7	0.7	6.0	10.0	8.0	4.0			D 28.667	1	
ARG	196	12.7			0.7			2.7	0.7	0.7	0.7					13.3	60.0	4.0	3.3	1.3		R 60.000	7	
ALA	197	18.0			12.7	18.7		0.7	3.3		2.0			29.3	3.3	0.7	6.0	5.3				P 29.333	1	
GLY	198	1.3						98.7														G 98.667	9	
VAL	199					5.3			47.3		12.0								30.7	4.7		I 47.333	5	
THR	200	5.3	0.7	0.7	2.0			3.3	2.0	3.3	1.3	2.7		1.3		10.0	8.0	8.7	35.3	14.7	0.7	T 35.333	1	
PRO	201	6.0	0.7			22.0		2.7	16.7	0.7	7.3			4.0		1.3	1.3	0.7	32.7	4.0		V 32.667	5	
ASN	202	7.3			2.0	5.3	0.7	10.7	17.3	4.0	0.7	18.7	0.7	14.0	0.7	6.0	2.7	1.3	1.3	5.3	1.3	L 18.667	1	
ASP	203	2.7			50.7	1.3		17.3	10.7					7.3	2.7	4.0	1.3	1.3			0.7	D 50.667	3	
ASP	204				95.3			1.3						3.3								D 95.333	9	
TRP	205	2.0						1.3											96.7			W 96.667	9	
ALA	206	2.0			80.7	0.7			2.7		0.7			12.0			1.3					D 80.667	7	
ALA	207	15.3						14.0	0.7					55.3	7.3		4.7	2.0		0.7		N 55.333	8	
ILE	208					18.0			39.3		16.7	20.7							5.3			I 39.333	6	
GLY	209							100.0														G 100.000	9	
MET	210										6.0	2.0			92.0							Q 92.000	9	
ARG	211									2.0							96.7		1.3			R 96.667	9	
GLN	212	0.7	0.7									37.3				50.7	2.7		7.3	0.7		Q 50.667	9	
THR	213	3.3																12.0	84.7			T 84.667	9	
ASP	214	22.0			54.0	16.0		6.0										0.7		1.3		D 54.000	8	
SER	215					0.7		2.7											96.7			S 96.667	9	
GLY	216				1.3			97.3						1.3								G 97.333	9	
SER	217	1.3						10.0						4.0		0.7	1.3	52.7	30.0			S 52.667	7	
THR	218	4.7				1.3			5.3		0.7						2.7	2.7	82.0	0.7		V 82.000	8	
ASP	219	2.0			4.0	17.3	1.3	0.7	6.0	4.7	5.3	2.0	2.7		3.3	15.3	10.7	18.0	6.7			T 18.000	1	
PHE	220						74.0			12.0	10.7								1.3	2.0		F 74.000	8	
HIS	221	4.7			28.0	29.3			8.7		4.0			9.3		2.7	4.7	1.3	4.0	3.3		E 29.333	2	
ASN	222	4.7			24.7	0.7		14.0	1.3	4.7				21.3		12.0	12.7	4.0				D 24.667	2	
VAL	223	2.7				4.0			1.3		2.7							2.7	86.0	0.7		V 86.000	9	
LYS	224	6.7				8.7	2.7		2.0	0.7	6.7	8.0			12.7	2.0	37.3	2.7	4.7	4.7	0.7	R 37.333	1	
VAL	225	3.3						15.3			13.3							2.0	66.0			V 66.000	6	
GLU	226	12.0			6.0	24.0	2.0	2.7	2.7		3.3	2.7		23.3	1.3	6.0	4.0	3.3		6.7		E 24.000	1	
PRO	227	18.9			10.1	12.8	0.7	1.4	6.1		5.4	0.7		2.0	16.2	0.7	6.1	2.0	1.4	0.7	14.9	A 18.919	1	
ASP	228	12.8			35.1	12.2	0.7	3.4	8.1		2.7	0.7		4.1		1.4	1.4	13.5	3.4	0.7		D 35.135	1	
GLU	229	7.3			22.7	50.0			1.3			1.3		1.3		4.7	6.0	4.0		1.3		E 50.000	6	
VAL	230	15.3	0.7			4.7			18.0		18.7	1.3					1.3		40.0			V 40.000	6	
LEU	231	7.3				4.0			5.3		78.0	0.7							4.7			L 78.000	7	
GLY	232	5.3			2.0	0.7	1.3	42.7	4.0	1.3	1.3	13.3		1.3	8.7	6.0	2.0	3.3	4.7	2.0		G 42.667	3	
ALA	233	10.2	0.7		12.2	6.1	6.8	2.7	6.1			2.0	0.7	6.8	9.5	2.7	6.8	8.2	0.7	4.1	8.2	D 12.245	1	
PRO	234	4.1			8.8	2.0	0.7	3.4	8.8	0.7	0.7	9.5		0.7	43.2	1.4	1.4	4.1	1.4	8.8	0.7	P 43.243	4	
ASN	235	8.8			14.3	8.2		32.7	1.4			6.8		2.0	9.5	0.7	1.4	8.2	3.4	2.7		G 32.653	1	
ALA	236	15.4			3.7	7.4	2.9	0.7	2.9	1.5	8.1	2.2		1.5	24.3	8.1	2.9	6.6	7.4	4.4		P 24.265	1	
PHE	237	6.9			6.2	6.9	1.5	4.6		1.5	3.8	21.5		2.3	18.5	4.6	1.5	6.2	7.7	3.8	0.8	1.5	L 21.538	1
VAL	238	6.2			8.5	6.2	8.5	10.0		0.8	9.2	2.3		0.8	13.1	1.5	0.8	23.8	3.8	2.3	1.5	0.8	S 23.846	2
LEU	239	15.4			13.5	3.8		11.5		17.3	1.9		1.9	3.8	17.3	7.7		3.8	1.9			KQ 17.308	1	
ALA	240	17.6			5.9	7.8			2.0					45.1			7.8	7.8	5.9			P 45.098	2	

PHE	241		50.0		16.7			16.7	8.3									D	50.000	3*				
ILE	242							15.4	76.9		7.7							L	76.923	6				
GLN	243	5.4			3.6	7.1		3.6	16.1	1.8	16.1	5.4	5.4	12.5	19.6	3.6		T	19.643	1				
SER	244	1.3		3.3	4.7	6.7	0.7	2.0	4.7	2.0	2.7		2.7	4.0		7.3	22.0	34.7	1.3	T	34.667	4		
GLU	245	8.0		1.3	3.3	0.7	0.7	0.7	1.3		1.3		59.3	2.7	4.7	0.7	2.0	12.7		0.7	P	59.333	4	
ARG	246	2.0			34.7	6.0	0.7	0.7	0.7	0.7	4.7			4.0	26.0	1.3		0.7	2.0	16.7	F	34.667	4	
GLY	247	40.0		4.0	2.7		3.3	1.3	2.0	0.7			8.0	9.3	5.3	0.7	17.3	4.0	1.3		A	40.000	4	
SER	248	4.0	10.7			4.0	0.7				1.3			9.3		24.7	45.3				T	45.333	6	
LEU	249		0.7			8.0		3.3	83.3	0.7							0.7	3.3			L	83.333	8	
PHE	250	4.0	0.7	1.3		2.0	0.7	6.7	3.3		8.7		12.7		46.7	1.3	2.0	10.0			R	46.667	6	
ALA	251	10.7			0.7	10.0		0.7	8.0		3.3	20.7			14.0	22.0	10.0				T	22.000	5	
PRO	252	6.0	7.3				2.0	2.7	34.0	2.7	34.7	7.3			1.3	1.3		0.7			P	34.667	5	
ILE	253	6.0			6.0	3.3	4.0	20.7	26.7	0.7		1.3		0.7	12.0	18.0		0.7			L	26.667	3	
ALA	254	39.3			4.0	5.3	1.3	22.0	0.7	0.7		4.7		14.7	2.7	0.7	4.0				A	39.333	7	
GLN	255						1.3					94.7	3.3					0.7			Q	94.667	9	
LEU	256	4.7					3.3		81.3	0.7		0.7		8.0	0.7	0.7					L	81.333	7	
ILE	257	6.0			0.7	2.0	26.7		10.7	1.3	2.7			0.7	3.3	46.0					V	46.000	6	
PHE	258				40.7		6.7	2.0	2.0	40.0	3.3		1.3	0.7	3.3						F	40.667	8	
ALA	259	31.3				4.0		2.7	4.0					9.3	20.7	28.0					A	31.333	5	
ASN	260	8.7	0.7		2.7	0.7		14.0		0.7		59.3		8.0	0.7	2.7	0.7			1.3	N	59.333	7	
VAL	261				27.3			27.3	30.0	3.3							12.0				L	30.000	6	
TYR	262	0.7	2.7	8.0		20.0			4.0					1.3					63.3		Y	63.333	7	
LEU	263	10.0						10.0	58.7				0.7			1.3	19.3				L	58.667	6	
GLY	264	3.3				96.7															G	96.667	9	
ILE	265							64.0	7.3	2.0	3.3			6.0	12.0	5.3					I	64.000	8	
ALA	266	92.0				5.3								1.3	0.7	0.7					A	92.000	9	
HIS	267	3.3		0.7	53.3	0.7	2.7	2.7	0.7	0.7	6.0	0.7		18.7	6.0	1.3	0.7	0.7	1.3		E	53.333	5	
GLY	268	2.7		0.7		96.0					0.7										G	96.000	8	
ALA	269	92.0				1.3		1.3	0.7						1.3	0.7	2.7				A	92.000	9	
LEU	270		0.7		23.3		0.7	0.7	72.0			1.3	0.7			0.7					L	72.000	7	
ASP	271	28.0		16.0	24.7		0.7	0.7	0.7	4.0		2.7		11.3	4.0	2.7	4.0	0.7			A	28.000	1	
ALA	272	22.0		5.3	44.0	4.7	0.7	0.7			0.7			7.3	1.3	0.7	8.7	3.3		0.7	E	44.000	4	
ALA	273	91.3			0.7	6.7										0.7	0.7				A	91.333	9	
ARG	274	14.7	1.3		0.7	0.7		1.3	2.0	12.7	13.3		1.3	0.7	36.0	7.3	1.3	6.0	0.7		R	36.000	4	
GLU	275	10.7		22.0	27.3		4.0	4.0	6.0			2.7	1.3	6.0	11.3	2.0	2.7				E	27.333	1	
TYR	276	1.3			12.0		2.7		2.0	1.3				1.3		2.0			4.7	72.7	Y	72.667	7	
THR	277	2.0			1.3	0.7		2.7	4.0						2.7	62.0	24.7				T	62.000	7	
ARG	278	2.7			0.7	2.7		6.0	17.3	0.7	1.3		4.7	50.0	2.0	6.0	6.0				R	50.000	4	
THR	279	12.3		6.2	15.8		2.1	2.1	8.2	2.7	2.1		3.4	5.5	4.1	35.6					T	35.616	2	
GLN	280	4.7		1.3	13.3		2.7	9.3	12.0		5.3		14.7	9.3	8.7	14.7	1.3	1.3	1.3		Q	14.667	1	
ALA	281	20.1		0.7		11.4	2.0	0.7	0.7			1.3	2.7	3.4	23.5	31.5	2.0				T	31.544	5	
ARG	282	0.7			1.4			8.1		0.7			2.7	79.7	6.1		0.7				R	79.730	8	
PRO	283	23.0				0.7		0.7				73.0			2.0		0.7				P	72.973	6	
TRP	284				2.0										0.7			97.3			W	97.279	9	
THR	285	3.4		4.1	20.4	0.7	4.8	16.3	0.7	12.9	1.4		17.7	2.0	1.4	2.7	2.0	8.8		0.7	F	20.408	2	
PRO	286	16.8		2.7	10.1	5.4	2.0	9.4	0.7	3.4	8.1	1.3	2.0	4.0	3.4	4.7	15.4	2.0		8.7	A	16.779	3	
ALA	287	14.7		1.3	0.7	0.7	13.3					0.7			66.7	2.0					S	66.667	7	
GLY	288	2.7		6.7	0.7		67.3	2.0	0.7	0.7	3.3		4.0	2.0	1.3	0.7	3.3	2.0		2.0	0.7	G	67.333	2
ILE	289	16.0		9.3	2.0	1.3		2.0	2.0		6.7		3.3		0.7	2.7	0.7	52.7		0.7	V	52.667	5	
GLN	290	16.0		16.7	42.7		0.7	0.7		0.7		2.7	0.7	7.3	1.3	4.7	4.0	1.3		0.7	E	42.667	1	
GLN	291	5.3	0.7	4.7	3.3		2.0	4.7	0.7	6.7	0.7		0.7	8.7	34.7	16.7	10.7				R	34.667	1	
ALA	292	69.3				3.3	5.3	1.3	0.7		0.7	4.7	0.7		5.3	2.7	4.7		1.3		A	69.333	7	
THR	293	16.7		0.7	3.3		4.7	2.0	4.7	0.7	0.7		2.0	3.3	5.3	4.0	12.7	23.3	16.0		T	23.333	1	
GLU	294	2.7		46.0	28.7		0.7	1.3	0.7	1.3		3.3		12.7	2.0		0.7				D	46.000	4	
ASP	295	0.7		84.0	14.7							0.7									D	84.000	9	
PRO	296				7.3	0.7	0.7		0.7			86.7		0.7			0.7	2.7			P	86.667	8	
TYR	297				6.0	0.7	1.3		13.3				2.0					4.7	72.0		Y	72.000	7	
THR	298	2.0				3.3	39.3		13.3	0.7	1.3		1.3			10.7	28.0				I	39.333	4	
ILE	299	0.7				0.7	10.7	2.7	58.7				19.3	3.3			4.0				L	58.667	6	
ARG	300	10.7		4.7	18.0		3.3	8.7	4.0	4.0		0.7		18.7	15.3	4.7	3.3	2.7		1.3	Q	18.667	4	
SER	301	5.3		0.7	0.7		4.7	24.0	1.3	3.3	6.7		2.0	4.0	32.7	0.7	12.0	2.0			R	32.667	4	
TYR	302	2.7			25.3		0.7	2.0	3.3	0.7							0.7	8.0		56.7	Y	56.667	5	

GLU 365		16.0	78.0						6.0						E 78.000	8		
VAL 366	10.7			2.0	0.7	6.7	22.7	0.7	1.3	0.7		0.7	53.3	0.7	V 53.333	6		
ILE 367	10.0	5.3			1.3	2.7	4.7	20.0	4.0		4.0	42.7	5.3		T 42.667	6		
GLY 368					100.0										G 100.000	9		
ALA 369	80.0				1.3				0.7			6.7	11.3		A 80.000	8		
ARG 370	1.3	0.7		0.7	0.7	2.7	0.7		0.7	88.0	4.0	0.7			R 88.000	8		
GLY 371	57.3				4.7						36.0	1.3		0.7	A 57.333	7		
THR 372	16.7						1.3					3.3	78.0	0.7	T 78.000	5		
HIS 373	36.0	0.7		0.7	14.0	2.0	8.0	1.3	0.7	1.3	0.7	16.7	16.0	2.0	A 36.000	8		
PRO 374	37.3	4.7	1.3	4.0	1.3	0.7	1.3	2.0	12.7	1.3	1.3	7.3	17.3	6.7	0.7	A 37.333	4	
ARG 375	19.3	2.7	2.0	6.0	3.3	22.0			0.7	8.0	5.3	12.0	18.0	0.7	K 22.000	2		
TYR 376	2.7		1.3	6.7		7.3		36.0	2.7		0.7	2.0	1.3	14.0	25.3	L 36.000	3	
GLY 377	4.7	0.7			67.3	0.7			10.7			16.0			G 67.333	7		
PHE 378				37.3		0.7		55.3	1.3					1.3	4.0	L 55.333	5	
ASP 379		93.3				6.0			0.7						D 93.333	9		
ARG 380					0.7	4.7	3.3				90.7			0.7	R 90.667	9		
PHE 381			60.7		20.0										19.3	F 60.667	6	
TRP 382			0.7												99.3	W 99.333	9	
ARG 383										100.0						R 100.000	9	
ASN 384		16.0						84.0								N 84.000	9	
VAL 385	32.7				8.0	24.0			0.7				34.7		V 34.667	7		
ARG 386										100.0						R 100.000	9	
THR 387				2.0		0.7						82.7	14.7		T 82.667	9		
HIS 388		4.0		80.0		6.0			9.3						0.7	H 80.000	9	
SER 389											15.3	84.7				T 84.667	9	
LEU 390							94.0					2.0	4.0		L 94.000	9		
HIS 391	0.7				96.7					0.7				2.0	H 96.667	9		
ASP 392		90.7	2.7					6.0						0.7	D 90.667	9		
PRO 393									98.7	0.7		0.7			P 98.667	9		
VAL 394	10.1				12.1	20.1			0.7			1.3	55.7		V 55.705	6		
SER 395	23.5	42.3	7.4	4.7	0.7				2.7	2.0	8.1	4.7	0.7	3.4	D 42.282	7		
TYR 396					5.4				1.3				0.7	8.1	84.6	Y 84.564	8	
LYS 397						85.2				14.8					K 85.235	9		
ILE 398	16.1	0.7	0.7	0.7	14.8	4.7	28.9	6.0	2.7	6.7	1.3	2.7	10.1	4.0	L 28.859	3		
ALA 399	2.7				5.4	0.7	8.7	2.7	0.7	15.4	61.1	0.7	0.7	0.7	0.7	R 61.074	6	
ASP 400	4.0	25.5	54.4	0.7	6.7		0.7	3.4	0.7			3.4	0.7		E 54.362	8		
VAL 401					19.5	37.6								43.0	V 42.953	7		
GLY 402					100.0										G 100.000	9		
LYS 403	7.4	21.5	13.4			2.7	0.7	9.4	5.4	34.2	1.3	2.7	1.3		R 34.228	4		
HIS 404	0.7		15.4		18.1									40.3	25.5	W 40.268	4	
THR 405	41.6		1.3	10.7		0.7	10.1	0.7		4.7	1.3		5.4	20.1	3.4	A 41.611	5	
LEU 406			0.7			1.3	95.3						0.7	2.0		L 95.302	9	
ASN 407	0.7	3.4	1.3		1.3	1.3	2.0	12.8	43.0		3.4	7.4	23.5		N 42.953	5		
GLY 408	1.3	14.1	3.4	60.4	3.4				4.0	5.4	6.0	1.3			0.7	G 60.403	1	
GLN 409	9.4	2.7	25.5		1.3	3.4	5.4	0.7	1.3	0.7	12.8	12.1	2.7	16.1	6.0	E 25.503	1	
TYR 410	6.1		0.7	7.5	8.8	10.2	1.4	21.8		4.8	9.5	0.7		13.6	1.4	13.6	L 21.769	1
PRO 411									100.0							P 100.000	9	
ILE 412	10.8	5.9	36.3		2.9	5.9	8.8	2.0	2.0	2.0	1.0	2.0	2.9	13.7	3.9	E 36.275	1	
PRO 413	2.2		1.1		1.1				94.6			1.1				P 94.565	8	
GLY 414	2.6	1.3			11.8				2.6		3.9	39.5	38.2			S 39.474	6	
PHE 415			70.2	2.1	4.3	4.3								2.1	17.0	F 70.213	6	
THR 416													6.5		93.5	Y 93.548	8	
SER 417										100.0						S 100.000	6*	

References

1. Guan, L. J.; Lee, W. C.; Wang, S.; Ohshiro, T.; Izumi, Y.; Ohtsuka, J.; Tanokura, M., Crystal structures of apo-DszC and FMN-bound DszC from *Rhodococcus erythropolis* D-1. *Febs J* **2015**, *282*, 3126-35.
2. Hino, T.; Hamamoto, H.; Suzuki, H.; Yagi, H.; Ohshiro, T.; Nagano, S., Crystal structures of TdsC, a dibenzothiophene monooxygenase from the thermophile *Paenibacillus* sp A11-2, reveal potential for expanding its substrate selectivity. *J Biol Chem* **2017**, *292*, 15804-15813.
3. Sondergaard, C. R.; Olsson, M. H. M.; Rostkowski, M.; Jensen, J. H., Improved Treatment of Ligands and Coupling Effects in Empirical Calculation and Rationalization of pK_a Values. *J Chem Theor Comp* **2011**, *7*, 2284-2295.
4. Zgarbova, M.; Otyepka, M.; Sponer, J.; Mladek, A.; Banas, P.; Cheatham, T. E.; Jurecka, P., Refinement of the Cornell et al. Nucleic Acids Force Field Based on Reference Quantum Chemical Calculations of Glycosidic Torsion Profiles. *J Chem Theor Comp* **2011**, *7*, 2886-2902.
5. Wang, J. M.; Wolf, R. M.; Caldwell, J. W.; Kollman, P. A.; Case, D. A., Development and testing of a general amber force field. *J Comput Chem* **2004**, *25*, 1157-1174.
6. Frisch, M. J.; Trucks, G. W.; Schlegel, H. B.; Scuseria, G. E.; Robb, M. A.; Cheeseman, J. R.; Scalmani, G.; Barone, V.; Mennucci, B.; Petersson, G. A.; Nakatsuji, H.; Caricato, M.; Li, X.; Hratchian, H. P.; Izmaylov, A. F.; Bloino, J.; Zheng, G.; Sonnenberg, J. L.; Hada, M.; Ehara, M.; Toyota, K.; Fukuda, R.; Hasegawa, J.; Ishida, M.; Nakajima, T.; Honda, Y.; Kitao, O.; Nakai, H.; Vreven, T.; Montgomery Jr., J. A.; Peralta, J. E.; Ogliaro, F.; Bearpark, M. J.; Heyd, J.; Brothers, E. N.; Kudin, K. N.; Staroverov, V. N.; Kobayashi, R.; Normand, J.; Raghavachari, K.; Rendell, A. P.; Burant, J. C.; Iyengar, S. S.; Tomasi, J.; Cossi, M.; Rega, N.; Millam, N. J.; Klene, M.; Knox, J. E.; Cross, J. B.; Bakken, V.; Adamo, C.; Jaramillo, J.; Gomperts, R.; Stratmann, R. E.; Yazyev, O.; Austin, A. J.; Cammi, R.; Pomelli, C.; Ochterski, J. W.; Martin, R. L.; Morokuma, K.; Zakrzewski, V. G.; Voth, G. A.; Salvador, P.; Dannenberg, J. J.; Dapprich, S.; Daniels, A. D.; Farkas, Ö.; Foresman, J. B.; Ortiz, J. V.; Cioslowski, J.; Fox, D. J. *Gaussian 09*, Gaussian, Inc.: Wallingford, CT, USA: Gaussian, Inc., 2009.
7. Jorgensen, W. L.; Chandrasekhar, J.; Madura, J. D.; Impey, R. W.; Klein, M. L., Comparison of Simple Potential Functions for Simulating Liquid Water. *J Chem Phys* **1983**, *79*, 926-935.
8. Becke, A. D., Density-Functional Exchange-Energy Approximation with Correct Asymptotic-Behavior. *Phys Rev A* **1988**, *38*, 3098-3100.
9. Becke, A. D., Density-functional thermochemistry. III. The role of exact exchange. *J Chem Phys* **1993**, *98*, 5648-5652.
10. Becke, A. D., Density-functional thermochemistry. IV. A new dynamical correlation functional and implications for exact-exchange mixing. *J Chem Phys* **1996**, *104*, 1040-1046.
11. Hariharan.Pc; Pople, J. A., Influence of Polarization Functions on Molecular-Orbital Hydrogenation Energies. *Theoret Chim Acta* **1973**, *28*, 213-222.
12. Hariharan, P. C.; Pople, J. A., Accuracy of Ah Equilibrium Geometries by Single Determinant Molecular-Orbital Theory. *Mol Phys* **1974**, *27*, 209-214.
13. Hehre, W. J.; Ditchfield, R.; Pople, J. A., Self-Consistent Molecular-Orbital Methods .12. Further Extensions of Gaussian-Type Basis Sets for Use in Molecular-Orbital Studies of Organic-Molecules. *J Chem Phys* **1972**, *56*, 2257-+.
14. Lee, C.; Yang, W.; Parr, R. G., Development of the Colle-Salvetti correlation-energy formula into a functional of the electron density. *Phys Rev B* **1988**, *37*, 785-789.
15. Miehlich, B.; Savin, A.; Stoll, H.; Preuss, H., Results Obtained with the Correlation-Energy Density Functionals of Becke and Lee, Yang and Parr. *Chem Phys Lett* **1989**, *157*, 200-206.
16. Vosko, S. H.; Wilk, L.; Nusair, M., Accurate Spin-Dependent Electron Liquid Correlation Energies for Local Spin-Density Calculations - a Critical Analysis. *Can J Phys* **1980**, *58*, 1200-1211.
17. Calixto, A. R.; Brás, N. F.; Fernandes, P. A.; Ramos, M. J., Reaction Mechanism of Human Renin Studied by Quantum Mechanics/Molecular Mechanics (QM/MM) Calculations. *ACS Catal* **2014**, *4*, 3869-3876.
18. Neves, R. P. P.; Fernandes, P. A.; Ramos, M. J., Unveiling the Catalytic Mechanism of NADP⁺-Dependent Isocitrate Dehydrogenase with QM/MM Calculations. *ACS Catal* **2016**, *6*, 357-368.

19. Ribeiro, A. J. M.; Yang, L.; Ramos, M. J.; Fernandes, P. A.; Liang, Z.-X.; Hirao, H., Insight into Enzymatic Nitrile Reduction: QM/MM Study of the Catalytic Mechanism of QueF Nitrile Reductase. *ACS Catal* **2015**, *5*, 3740-3751.
20. Gesto, D. S.; Cerqueira, N. M. F. S. A.; Fernandes, P. A.; Ramos, M. J., Unraveling the Enigmatic Mechanism of L-Asparaginase II with QM/QM Calculations. *J Am Chem Soc* **2013**, *135*, 7146-7158.
21. Seeger, R.; Pople, J. A., Self-Consistent Molecular-Orbital Methods .18. Constraints and Stability in Hartree-Fock Theory. *J Chem Phys* **1977**, *66*, 3045-3050.
22. Bauernschmitt, R.; Ahlrichs, R., Stability analysis for solutions of the closed shell Kohn-Sham equation. *J Chem Phys* **1996**, *104*, 9047-9052.
23. Schlegel, H. B.; McDouall, J. J. Do You Have SCF Stability and Convergence Problems? In *Computational Advances in Organic Chemistry*, Ögretir, C.; Csizmadia, I. G., Eds.; Kluwer Academic: The Netherlands, 1991; Vol. 330, pp 167-185.
24. Maseras, F.; Morokuma, K., Imomm - a New Integrated Ab-Initio Plus Molecular Mechanics Geometry Optimization Scheme of Equilibrium Structures and Transition-States. *J Comput Chem* **1995**, *16*, 1170-1179.
25. Singh, U. C.; Kollman, P. A., A Combined *Ab initio* Quantum-Mechanical and Molecular Mechanical Method for Carrying out Simulations on Complex Molecular-Systems - Applications to the CH₃Cl + Cl⁻ Exchange-Reaction and Gas-Phase Protonation of Polyethers. *J Comput Chem* **1986**, *7*, 718-730.
26. Field, M. J.; Bash, P. A.; Karplus, M., A Combined Quantum-Mechanical and Molecular Mechanical Potential for Molecular-Dynamics Simulations. *J Comput Chem* **1990**, *11*, 700-733.
27. Das, D.; Eurenus, K. P.; Billings, E. M.; Sherwood, P.; Chatfield, D. C.; Hodoscek, M.; Brooks, B. R., Optimization of quantum mechanical molecular mechanical partitioning schemes: Gaussian delocalization of molecular mechanical charges and the double link atom method. *J Chem Phys* **2002**, *117*, 10534-10547.